Formation mechanisms of oxygen atoms in the O($^1D_2$) state from the 157 nm photoirradiation of amorphous water ice at 90 K

Tetsuya Hama,[1] Akihiro Yabushita,[1] Masaaki Yokoyama,[1] Masahiro Kawasaki,[1,a)] and Naoki Watanabe[2]
[1]*Department of Molecular Engineering, Kyoto University, Kyoto 615-8510, Japan*
[2]*Institute of Low Temperature Science, Hokkaido University, Sapporo 060-0819, Japan*

(Received 6 April 2009; accepted 14 July 2009; published online 21 September 2009)

Vacuum ultraviolet photolysis of water ice in the first absorption band was studied at 157 nm. Translational and internal energy distributions of the desorbed species, O(^1D) and OH($v=0,1$), were directly measured with resonance-enhanced multiphoton ionization method. Two different mechanisms are discussed for desorption of electronically excited O(^1D) atoms from the ice surface. One is unimolecular dissociation of H_2O to H_2+O(^1D) as a primary photoprocess. The other is the surface recombination reaction of hot OH radicals that are produced from photodissociation of hydrogen peroxide as a secondary photoprocess. H_2O_2 is one of the major photoproducts in the vacuum ultraviolet photolysis of water ice. © *2009 American Institute of Physics*.
[doi:10.1063/1.3194798]

I. INTRODUCTION

The chemical and physical processes following the photodissociation of water ice have been extensively studied because of its importance to reaction dynamics and kinetics, the upper atmospheric chemistry and astrophysics. Photolysis in the first absorption band of water ice (130–165 nm) involves two primary processes,

$$H_2O + h\nu \rightarrow H_2 + O(^1D), \quad (1)$$

$$H_2O + h\nu \rightarrow H + OH. \quad (2)$$

O(^1D) from primary reaction (1) could be an efficient reactant in formation of complex molecules on interstellar ices because of its high reactivity even though this reaction may be a minor channel. For example, the CO_2 molecule is one of main components of ice mantle observed toward interstellar molecular clouds and requires surface reactions to attain the observed abundances. Because a large amount of solid CO exist on/in interstellar water ice,[1] one mechanism for CO_2 formation has been suggested to be the barrierless reaction of O(^1D) and CO: $CO+O(^1D)\rightarrow CO_2$.[2–6] Another CO_2 formation mechanism is the reaction of OH and CO: $CO+OH\rightarrow CO_2+H$ by overcoming the barrier height in the gas phase, 2.7 kcal/mol.[4–6]

In the gas phase, Stief *et al.*[7] reported the relative quantum yields for reaction (1) to be 0.11 for 105–145 nm and ≤0.01 for 145–185 nm, while Ung[8] estimated it to be 0.08 at 147 nm. In the condensed phase the O(^1D) formation reaction (1) has not been directly confirmed. In the photolysis of amorphous solid water (ASW) at the vacuum ultraviolet (vuv) region, the penetration depths are ~100 and ~35 nm for the first band at λ=157 and 140 nm, respectively, and ~50 nm for the second band at λ=122 nm.[9] Various photoproducts were detected in and on ice at 10 K.[10] The main photoproducts, OH, H_2O_2, and HO_2, were the primary and secondary photoproducts of reaction (2). In the condensed phase photolysis, not only the primary unimolecular reactions but also the secondary reactions would be the sources of photoproducts. Following the ultraviolet photolysis of H_2O_2 in various rare-gas matrices at 7.5 K, a (H_2O–O) complex was formed from the recombination of OH radicals, while the primary formations of H_2O+O(^1D) or O(^3P_J) have not been established from the photodissociation of gaseous H_2O_2 at 124–254 nm.[11,12] Experimental works on photon- or electron-stimulated desorption (ESD) of species from water ice have also been reported,[13–20] and their results showed various desorbing species such as H, H_2, OH, H_2O, and O_2. For example, Kimmel and Orlando[21] have used resonance-enhanced multiphoton ionization (REMPI) to study the ESD of O atoms in the ^1D and ^3P states from amorphous D_2O.

In the present study, using pulsed 157 nm (181 kcal/mol) laser radiation the desorptions of electronically excited O(^1D) atoms via the primary and secondary photoprocesses from ASW at 90 K have been directly confirmed by REMPI. Translationally and internally excited OH formation mechanisms were also discussed since hot OH is a plausible source for the oxygen atom.

II. EXPERIMENTAL

A. Apparatus and preparation of ice films

Experimental details are described elsewhere.[22] ASW was prepared by backfilling deposition of water vapor onto a sapphire disc substrate sputter coated with a thin polycrystalline film of Au(111) at 90 K for 60 min by a pulsed nozzle (General Valve) at rate of 10 Hz and at 20 Torr stagnation pressure of water vapor. In order to spread water vapor all over the chamber, a flat plate was attached in front of the

a)Author to whom correspondence should be addressed. Electronic addresses: kawasaki@moleng.kyoto-u.ac.jp. FAX: +81-75-383-2573.

pulse nozzle. The exposure was typically 1500 L (1 L=1 $\times 10^{-6}$ Torr s). This exposure resulted in formation of 500 monolayers (ML) of H_2O on the substrate if we adopt the reported experimental conversion factor of 1 ML deposition by 3 L exposure.[23]

Unfocused 157 nm laser radiation with full width at half maximum duration of 10 ns was incident at an angle of about 80° to the surface normal on the ice surface at a fluence <0.1 mJ cm^{-2} pulse^{-1}. O(^1D) atom products were subsequently ionized at a distance of 4 mm (2 mm for OH) from the substrate surface by the (2+1) REMPI transition via the O($^1F_3 \leftarrow {}^1D_2$) transition at 203.8 nm,[24] and collected with a small mass spectrometer aligned perpendicular to the ice surface. O(^1D) atoms were also observed via the O($^1P_1 \leftarrow {}^1D_2$) transition at 205.5 nm.[25] OH($v=0$ and 1) products were also detected by REMPI via the $D\ ^2\Sigma^-(v'=0) \leftarrow X\ ^2\Pi(v''=0)$ at 243.5–245.0 nm and the $3\ ^2\Sigma^-(v'=0) \leftarrow X\ ^2\Pi(v''=1)$ transitions at 237.5–237.7 nm, respectively. The REMPI transition strength data are obtained by Greenslade *et al.*[26] The delay t between the photolysis and REMPI laser pulses was varied with a delay generator to allow investigation of the flight times of the photoproducts. Three types of ice samples, fresh ASW, ASW after 157 nm photoirradiation for 30 min, and fresh H_2O_2 on ASW, were prepared. The surface of fresh ASW was kept fresh for laser irradiation by expanding water vapor to the ASW surface by a pulsed nozzle at rate of 10 Hz. The duration of the H_2O pulse was about one millisecond. During this exposure, the chamber pressure was increased up to 5 $\times 10^{-7}$ Torr. For the concentrated H_2O_2 photolysis experiments, a commercially available H_2O_2 solution (30%) was concentrated in a glass container by vacuum distillation and the H_2O_2/H_2O vapor was deposited on the gold substrate. The exposure of the codeposited H_2O_2/H_2O mixture on the ASW film was <8 L for 330 s duration at 90 K. Fresh surfaces of cocondensed H_2O_2 were prepared as described above. The photolysis experiments were performed at 90 K.

B. Simulation of time-of-flight spectra of photoproducts

The measured time-of-flight (TOF) spectra were fitted with one or more flux-weighted Maxwell–Boltzmann (MB) distributions defined by a translational temperature T_{trans}. Details regarding the simulation of such TOF spectra have been reported previously.[22] The TOF spectrum $S(a_i,t,T_{trans})$ was fitted with a combination of the MB distributions defined by the temperature T_{trans}. The coefficient a_i is used for the relative population of each MB distribution,

$$S(a_i,t,T_{trans}) = \Sigma a_i S_{MB}(t,T_{trans}), \quad (3)$$

$$S_{MB}(t,r) = r^3 t^{-4} \exp[-mr^2/2k_B T_{trans} t^2], \quad (4)$$

$$P_{MB}(E_t) = (k_B T_{trans})^{-2} E_t \exp[-E_t/k_B T_{trans}], \quad (5)$$

where r is a flight length for the photofragment. The MB distribution $P_{MB}(E_t)$ as a function of translational energy E_t is characterized by the averaged translational energy $\langle E_t \rangle = 2k_B T_{trans}$, where k_B is the Boltzmann constant.[27] Conversion from the energy distribution to the TOF distribution was performed using the Jacobian listed by Zimmerman and Ho.[28]

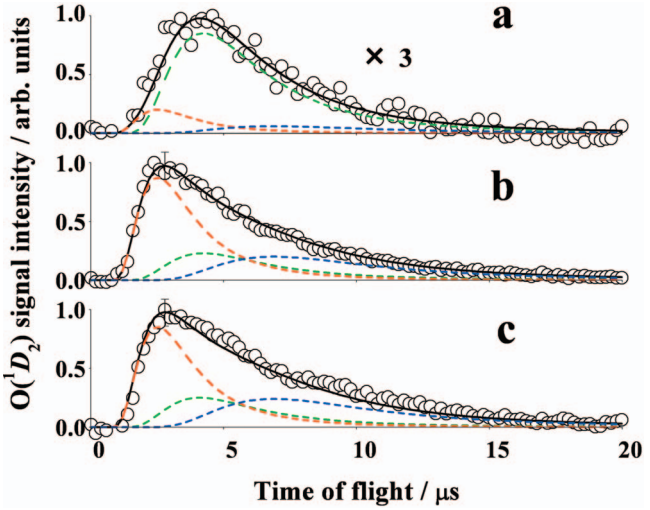

FIG. 1. TOF spectra of O(^1D) atoms from the 157 nm photodissociation of (a) fresh ASW at 90 K, (b) ASW after photoirradiation for 30 min, and (c) fresh H_2O_2 on ASW. Translational temperatures and contributions are listed in Table I.

III. RESULTS

A. TOF spectra of O(^1D) atoms

Figure 1 shows TOF spectra of the O($^1F_3 \leftarrow {}^1D_2$) transition from the photodissociation of (a) fresh ASW, (b) ASW after 157 nm photoirradiation for 30 min without intermissive dosing of water vapor, and (c) fresh H_2O_2 on ASW. These TOF spectra are reproduced by three MB distributions with $T_{trans}=2250\pm250$ K ($\langle E_{trans}\rangle=9.0\pm1.0$ kcal/mol), 800 ± 150 K (3.2 ± 0.6 kcal/mol), and 300 ± 100 K (1.2 ± 0.4 kcal/mol). For both cases (b) and (c), the stronger O(^1D) signals and the larger contributions of the O($^1D, T_{trans}=2250$ and 300 K) components were observed than those for case (a). Table I summarizes the results.

B. O(^1D) signal intensity change as a function of 157 nm photoirradiation time

Figure 2 shows the O($^1F_3 \leftarrow {}^1D_2$) transition signal intensity change as a function of the 157 nm irradiation time for the O($^1D, T_{trans}=2250$ and 300 K) atoms. In Fig. 2, the pre-

TABLE I. Contributions (%) of translational temperature (T_{trans}) components of O(^1D) atoms from the 157 nm photolysis of ASW and hydrogen peroxide (H_2O_2) at 90 K.

Ice sample	T_{trans} (K) 2250	800	300	Relative integrated TOF signal intensity[a]
Fresh ASW[b]	11	80	9	1
ASW after photoirradiation[c]	49	22	29	3.5 ± 0.5
Fresh H_2O_2 on ASW	46	22	32	3.7 ± 0.3

[a]Integrated TOF signal intensities are relative to the fresh ASW sample.
[b]ASW stands for amorphous solid water at 90 K.
[c]After 30 min photoirradiation at 157 nm.

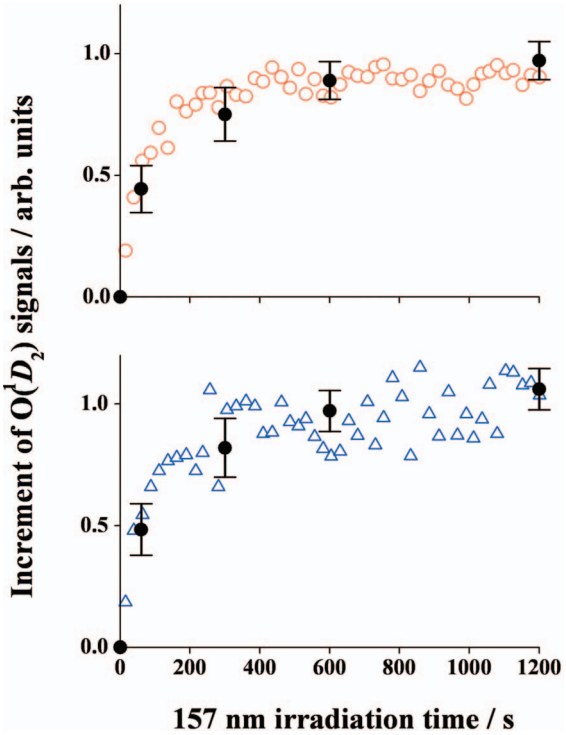

FIG. 2. Time evolution curves of the $O(^1D)$ signals at TOF=2 μs (upper panel, red open circles) and 10 μs (lower panel, blue open triangles) from ASW as a function of 157 nm irradiation time. The *y*-axis shows increment of the $O(^1D)$ signal intensities so that weak signals due to unimolecular dissociation reaction (6) are offset. Previously reported and presently measured time evolution of H_2O_2 photoproducts accumulated on ASW is represented by the filled circles (Ref. 29).

viously reported and presently measured time evolution data for the $R(1)+R(5)$ line of OH($v=0$) due to the H_2O_2 photoproduct on the 157 nm photoirradiated ASW surface are also plotted,[29] which reflects the concentration of photogenerated H_2O_2 on the ice surface. The appearance behaviors of the OH signal from the secondary photodissociation of H_2O_2 photoprepared on the ASW surface and the $O(^1D)$ signals in Fig. 2 were in agreement within the margin of error.

C. OH radical desorption in the 157 nm photoirradiation on amorphous solid water

Translationally and internally excited OH radicals have been successfully detected with the same REMPI setup following 157 nm photolysis of H_2O or H_2O_2 ices at 90 K, and the formation mechanisms were described before.[30] Only details relevant to the present experiments are given here. The upper panels of Fig. 3 show (a) TOF spectra of the $R(1)+R(5)$ line of OH($v=0$) and (b) the $R(2)$ line of OH($v=1$) following 157 nm photodissociation of fresh ASW. The lower panels are for (c) the $R(1)+R(5)$ line of OH($v=0$) at 244.25 nm and (d) the $R(2)$ line of OH($v=1$) at 237.62 nm following 157 nm photodissociation of ASW after photoirradiation for 30 min. The TOF spectra of OH are reproduced by two MB distributions with $T_{trans}=7500\pm1000$ (30 ± 4.0 kcal/mol) and 1300 ± 200 K (5.2 ± 0.8 kcal/mol). The population ratio of $v=1/v=0$ was estimated to be 0.2 ± 0.1 by REMPI transition strength data by Greenslade *et al.*[26] Observed rotational temperatures and

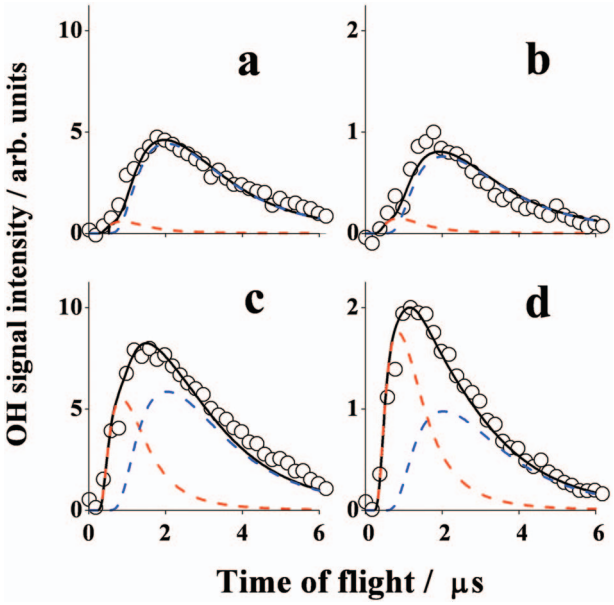

FIG. 3. Upper panels: TOF spectra of OH; (a) OH($v=0$) (b) OH($v=1$) from the 157 nm photodissociation of fresh ASW at 90 K. Lower panels; (c) OH($v=0$) and (d) OH($v=1$) from the 157 nm photodissociation of ASW after 30 min photoirradiation. Translational temperatures and contributions are listed in Table II.

vibrational level ratios of OH($v=0$ and 1) are listed in Table II. The TOF spectra of OH from fresh H_2O_2 on ASW were also measured, which were similar to those were obtained from the ASW after 30 min irradiation (not shown). For both cases, about two times stronger OH signal intensities and larger contributions of the OH($T_{trans}=7500$ K) component were obtained than those for the fresh ASW case. The maximum (kinetic+internal) energy of the observed OH formed by 157 nm photodissociation of ASW after photoirradiation for 30 min is about 55 kcal/mol.

IV. DISCUSSION

A. $O(^1D)$ formation mechanism in fresh ASW

As shown in Table I and Fig. 1, both the TOF spectra for ASW after photoirradiation and fresh H_2O_2 on ASW have similar translational distributions, that is, a smaller contribution of the middle temperature component ($T_{trans}=800$ K) and higher total signal intensities than those for fresh ASW. The TOF spectrum for fresh ASW consists mostly of the middle temperature component. Since this middle temperature component comes from the fresh water surface and not from the secondary photoproducts such as H_2O_2, we propose that the primary unimolecular process (6) results in the formation of this component,

$$H_2O(ads) + h\nu(157\ nm) \rightarrow H_2(i) + O(^1D). \quad (6)$$

The available energy for reaction (6) at 157 nm is $E_{avail}(6)=7.9$ kcal/mol. In the present paper, the notation "ads" stands for condensed phase or adsorbed state, and the thermodynamic data for adsorbed species are taken from those for the solid phase. The notation "i" stands for species at the ASW/vacuum interface, and for these species we use the gas phase thermodynamics data.[31,32] According to quantum me-

TABLE II. Translational and rotational temperatures (T_{trans} and T_{rot}) of OH($v=0$ and 1) radicals from three different ice samples.

Ice sample	T_{trans} (K)[a]		T_{rot} (K)[b]		Relative integrated TOF signal intensity[c]		Vibrational level ratio
	$v=0$	$v=1$	$v=0$	$v=1$	$v=0$	$v=1$	$v=1/v=0$[b]
Fresh ASW	7500 (5%) 1300 (95%)	7500 (10%) 1300 (90%)	400	300	1	1	0.2 ± 0.1
ASW after photoirradiation	7500 (30%) 1300 (70%)	7500 (40%) 1300 (60%)	500	200	1.7 ± 0.1	1.8 ± 0.1	0.2 ± 0.1
Fresh H_2O_2 on ASW	7500 (30%) 1300 (70%)	7500 (40%) 1300 (60%)	500	200	1.6 ± 0.1	1.7 ± 0.1	0.2 ± 0.1

[a]The percentage in parenthesis is a contribution of each temperature component.
[b]T_{rot} and the vibrational level ratios were measured at TOF=1.5 μs for fresh ASW and at TOF=0.5 μs for other two ice samples.
[c]Integrated TOF signal intensities are relative to the fresh ASW sample.

chanical wavepacket calculations for the photodissociation of water by van Harrevelt and van Hemert, the $H_2+O(^1D)$ channel occurs on the ground state potential surface that favors dissociation to H+OH.[33] Based on the experimental results for fresh ASW in Table I, most of the $O(^1D)$ atoms have the MB component with $T_{trans}=800$ K and are not totally accommodated to the surface temperature (90 K). These results suggest that the $O(^1D)$ atoms ejected from the surface would be produced on the ASW surface and not from the bulk,

$$\text{surface}-H_2O(\text{ads})+h\nu(157\ \text{nm})\rightarrow H_2(\text{i})+O(^1D). \quad (7)$$

Since the optical depth of ASW at 157 nm is about 100 nm, the 157 nm photons are primarily absorbed in the ASW bulk, and could induce several other possible mechanisms, including the diffusion of atoms, radicals, and molecules. However, $O(^1D)$ atoms generated in the bulk easily react with water molecules to produce OH radicals or H_2O_2 molecules by collisions and do not reach the surface.[34,35]

Concerning the exciton mediated reaction, Orlando and Kimmel have observed the ESD of O atoms in the ^1D and ^3P states from an amorphous D_2O film. O atoms in the ^1D and ^3P states were produced at threshold electron energies between 150 and 160 kcal/mol and desorbed with both the nonthermal (1.4–2.0 kcal/mol) and thermal components.[36] They associated the ESD of O atoms in the ^1D and ^3P states from ice with dissociation of the Frenkel-type excitons of $4a_1$ character, which are near the bottom of the ice conduction band. The excitons formed in the bulk ice are transported to the near-surface region, and then, the reduced forces in this region allow dissociation. There are both theoretical and experimental works which support the existence of mobile excitons in water ice. In the high-level electronic structure calculations, the lowest excited states of hydrogen-bonded water clusters (dimer, trimer, and pentamer) have the barrier for dissociation, and these results contrast with that of an isolated water molecule, in which the lowest excited state is well known to be dissociative.[37,38] Hahn *et al.* found that the exciton in ice showed significant overlap with adjacent sites.[39] These calculations imply that exciton would be prevented from dissociation within ASW, and in favor of dissociation at the vacuum/ASW interface after the migration. In fact, Petrik and Kimmel found experimental support for mobile excitons in ASW that initiate reactions at the ASW/vacuum interface.[40,41] This model could also be plausible for our experimental results that the $O(^1D)$ atom ejection occurs at the vacuum/ASW interface, that is, the dissociation of surface H_2O is the source of $O(^1D)$ atom.

We will describe below the other mechanism for $O(^1D)$ atom formation via recombination of OH radicals.

B. $O(^1D)$ formation mechanisms in ASW after 30 min photoirradiation and fresh H_2O_2 on ASW

As shown in Fig. 1 and Table I, the strong $O(^1D)$ signals and the large contributions of the $O(^1D, T_{trans}=2250$ and 300 K) components were observed in ASW after 157 nm photoirradiation for 30 min and fresh H_2O_2 on ASW. Figure 2 shows that the appearance behaviors of $O(^1D)$ signals at $t=2$ and 10 μs are in accordance with the concentration of photogenerated H_2O_2 on the ice surface. These results indicate that the $O(^1D, T_{trans}=2250$ and 300 K) atoms come from photogenerated H_2O_2. For the cases of both ASW after prolonged photoirradiation and fresh H_2O_2 on ASW, there are additional mechanisms for formation of $O(^1D)$ besides reaction (6); the collisional recombination reactions (11)–(14) of hot OH on the surface of ice,

$$H_2O(\text{ads})+h\nu(157\ \text{nm})\rightarrow H(\text{i})+OH(\text{i}), \quad (8)$$

$$OH(\text{i})+OH(\text{i and ads})\rightarrow H_2O_2(\text{ads}), \quad (9)$$

$$H_2O_2(\text{ads})+h\nu(157\ \text{nm})\rightarrow 2OH(\text{i}), \quad (10)$$

$$OH(\text{i})+OH(\text{i})\rightarrow H_2O(\text{i})+O(^1D) \quad (11)$$

$$\rightarrow H_2O(\text{ads})+O(^1D), \quad (12)$$

$$OH(\text{i})+OH(\text{ads})\rightarrow H_2O(\text{i})+O(^1D) \quad (13)$$

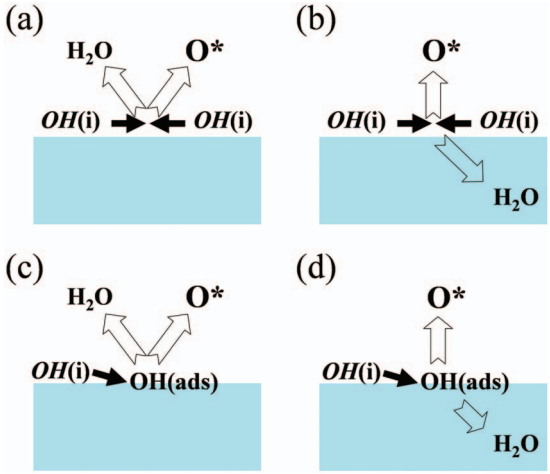

FIG. 4. Schematic illustrations of the OH recombination reactions on the surface. (a) Reaction (11), (b) reaction (12), (c) reaction (13), (d) reaction (14). *OH*(i) stands for hot OH radical at the ASW/vacuum interface, and OH(ads) for adsorbed species, and O* for $O(^1D)$ atom.

$$\rightarrow H_2O(ads) + O(^1D). \quad (14)$$

The schematic illustrations of reactions (11)–(14) are shown in Fig. 4. Thermodynamic data in units of kcal/mol are $E_{avail}(10)=115.9$, $\Delta_r H(11)=28.3$, $\Delta_r H(12)=17.6$, $\Delta_r H(13)=41.2$, and $\Delta_r H(14)=30.5$.[31,32] Reactions (11)–(14) are endothermic and barrierless processes.[42] The translational and internal energies of the OH radicals from ASW after prolonged 157 nm irradiation on ASW are in good accordance with those of the OH radicals from fresh H_2O_2 on ASW as shown in Table II. The translationally hot OH($v=0$ and $1, T_{trans}=7500$ K) from H_2O_2 would produce the $O(^1D)$ atoms via reactions (11)–(14). The energy available for the H_2O+O pair gains kinetic energy from the hot OH radicals and the O atom is provided with enough energy to be excited electronically.[11] Figure 4 shows that the hot OH radicals that can produce $O(^1D)$ atom could be formed from reaction (10). The large available energy in reaction (10) could accelerate $O(^1D)$ formation. Khriachtchev *et al.*[43] reported in their ultraviolet photolysis of H_2O_2 in low temperature Ar matrix that (a) the excess energy provides enough kinetic energy for, at least, one OH to exit the Ar matrix cage with some probability, and (b) a considerable part of the OH pairs that remain in the cage recombine to produce the H_2O-O van der Waals complex. The backreaction, $H_2O+O(^1D)\rightarrow H_2O_2$ was found in the matrix photolysis of a water-ozone mixture.[44] Andersson *et al.*[45,46] performed classical molecular dynamics calculations for photodissociation and photodesorption efficiencies of amorphous water ice at 10 K and predicted that the mobility of OH radicals is low within the ice. However, OH radicals formed in the top 3 ML are quite mobile on top of the surface and have an increased probability of reactions with other species in or on the ice. On the other hand, Petrik *et al.* reported the low-energy electron-stimulated production of molecular oxygen from ASW and proposed that the electron-stimulated migration of OH or OH^- to the vacuum interface where they react and produce molecular oxygen occurs via transport through the hydrogen bond network of the ASW.[17] Both models support that the recombination of OH occurs more readily at the surface of ASW compared to the bulk. In fact, Yabushita *et al.*[29] reported in their vuv photolysis experiments that H_2O_2 was subsequently produced on the water ice surface at 90 K presumably due to recombination of photolytically produced OH.

As for reaction (8), because of the momentum conservation between the H and OH photofragments, the OH radical is slowly moving. In addition, the vibrational state distribution $v=1/v=0$ of OH($v=0$ and 1) is ~0.2 in the condensed phase, which is much lower than the gas phase results of ~1.1 reported by Lu *et al.*,[47] Hwang *et al.*,[48] and Yang *et al.*[49] The vibrational energy of OH($v=1$) is 10.2 kcal/mol.[50] Andersson *et al.*[45,46] reported that the energy of the electronically excited state of H_2O was dissipated by the surrounding water molecules in the condensed phase, and this would lead to product energy distributions different from those if the excited molecule were unperturbed in the gas phase. Hence, reaction (9) mainly takes place from these low-energy OH radicals following the photolysis of H_2O.

The large contribution (80%) of $O(^1D, T_{trans}=800$ K) in fresh ASW shows that the $O(^1D)$ atoms are mainly formed via the primary unimolecular reaction (7) in fresh ASW. Table I shows the results of relative signal intensities of the $O(^1D, T_{trans}=800$ K) component for three ice samples. For fresh ASW, we have the relative $O(^1D)$ intensity $80(\%)\times 1=80$. For ASW after 157 nm photoirradiation and fresh H_2O_2 on ASW, we have the intensities $22(\%)\times 3.5=77$ and $22(\%)\times 3.7=81$, respectively. These results imply that the signal intensity of the $O(^1D, T_{trans}=800$ K) component did not change. Instead, the other components increased due to the bimolecular reactions (11)–(14) of hot OH radicals from the secondary photolysis of H_2O_2. A small contribution of the $O(^1D, T_{trans}=2250$ and 300 K) atoms in fresh ASW may be attributable to photogenerated H_2O_2 on ice because the intermissive water vapor deposition during the experiment did not perfectly cover the surfaces.

C. Transition state and reaction mechanism for the formation of $O(^1D)$ atoms via recombination reactions of OH radicals

Mousavipour and Saheb[42] performed theoretical calculations for the transition state of $H_2O+O(^1D)$ formation. According to them, in the kinetics and reaction mechanism of a hydroperoxyl radical (HO_2) with a H atom, reactions (15) and (16) proceed on a singlet surface to produce $H_2O+O(^1D)$ via the formation of intermediate oxywater (H_2OO),

$$H + HO_2 \rightarrow H_2OO, \quad (15)$$

$$H_2OO \rightarrow H_2O + O(^1D), \quad (16)$$

$$\text{net} \quad H + HO_2 \rightarrow H_2O + O(^1D). \quad (17)$$

Thermodynamic data in units of kcal/mol are $\Delta_r H(15)=-38.3$, $\Delta_r H(16)=36.0$, and $\Delta_r H(17)=\Delta_r H(15)+\Delta_r H(16)=-2.3$.[42]

H_2OO is a proposed structural isomer of hydrogen peroxide (HOOH), which may serve as a transient intermediate

in oxidation reactions initiated by hydrogen peroxide.[51,52] $O(^1D)$ atom can be produced without the barrier via the endothermic recombination reactions of hot OH radicals through the formation of HOOH and H_2OO,

$$OH + OH \rightarrow HOOH, \quad (18)$$

$$HOOH \rightarrow H_2OO, \quad (19)$$

$$H_2OO \rightarrow H_2O + O(^1D), \quad (20)$$

$$\text{net} \quad OH + OH \rightarrow H_2O + O(^1D). \quad (21)$$

Thermodynamic data in units of kcal/mol are $\Delta_r H(18) = -42.2$, $\Delta_r H(19) = 46.2$, and $\Delta_r H(20) = 36.0$ and $\Delta_r H(21) = \Delta_r H(18) + \Delta_r H(19) + \Delta_r H(20) = 40.0$.[42] The barrier height for reaction (19), $E_{\text{barrier}}(19)$, was calculated to be 52.2 kcal/mol.[42] Recently, Franz *et al.* reported an energy of 21 kcal/mol for the lowest electronic singlet states of H_2OO along dissociation of the oxygen-oxygen bond into H_2O and $O(^1D)$, reactions (16) or (20), with quantum chemical calculations.[53] When their value for $\Delta_r H(20) = 21.0$ kcal/mol is adopted, $\Delta_r H(21)$ is calculated as $\Delta_r H(21) = \Delta_r H(18) + \Delta_r H(19) + \Delta_r H(20) = 25.0$ kcal/mol, that is, much lower than the above listed value of 40.0 kcal/mol. In either case, this endothermic value is less than the maximum available energy, $E_{\text{avail}}(10)/2 = 58$ kcal/mol, for hot OH radical formation from the 157 nm photodissociation of H_2O_2. Actually the maximum (kinetic+internal) energy of the observed OH products from photogenerated H_2O_2 on ASW is about 55 kcal/mol.

We cannot identify particular mechanisms for the $O(^1D, T_{\text{trans}} = 2250$ and 300 K) atom formation. The two components of $O(^1D, T_{\text{trans}} = 2250$ and 300 K) atoms imply at least two reactions in reactions (11)–(14) can occur. Based on the fact that (a) the higher reactant energy from two hot OH and (b) the lowest value of $\Delta_r H(12)$, reaction (12) is the most plausible process.

D. Other mechanisms for $O(^1D)$ formation

One of the other possible mechanisms for $O(^1D)$ formation is the recombination reaction of H and OH,

$$H_2O(\text{ads}) + h\nu(157\ \text{nm}) \rightarrow H(\text{i}) + OH(\text{i}), \quad (22)$$

$$H(\text{i}) + OH(\text{i}) \rightarrow H_2(\text{i}) + O(^1D), \quad (23)$$

$$H(\text{i}) + OH(\text{ads}) \rightarrow H_2(\text{i}) + O(^1D), \quad (24)$$

$$H(\text{ads}) + OH(\text{i}) \rightarrow H_2(\text{i}) + O(^1D). \quad (25)$$

Thermodynamic data in units of kcal/mol are $E_{\text{avail}}(22) = 51.2$, $\Delta_r H(23) = 43.3$, $\Delta_r H(24) = 47.4$, and $\Delta_r H(25) = 56.2$.[31,32] There has been no direct measurement of $O(^1D)$ formation via the recombination reaction of H and OH in the gas phase. Since these reactions are largely endothermic and not three-body reactions, large rate reduction in these reaction rates would be expected on the surface. Classical molecular dynamics calculations for the condensed phase showed that a H_2O molecule was formed via H and OH recombination reaction following the photolysis of water ice.[45,46] Thus, the contribution of these reactions should be negligible.

Gerakines *et al.* reported the evolution of spectral features in vuv photoirradiation on H_2O ice and found that OH was the first photoproduct observed in ice at 10 K, and then, after OH, accumulation of H_2O_2 and HO_2 started.[10] In the present experiment, the contribution of the photolysis of OH(ads) for $O(^1D)$ formation, reaction (26), would be small in fresh ASW and H_2O_2 on ASW because it is unlikely that multiphoton process occurred with this low laser intensity of unfocused 157 nm laser at a fluence <0.1 mJ cm^{-2} pulse^{-1},[18,54] and also the surfaces of ice were kept fresh for laser irradiation by exposing them with water or H_2O_2/H_2O vapor to suppress the secondary photolysis of the accumulated products formed on the ice surface during the photolysis,

$$OH(\text{ads}) + h\nu(157\ \text{nm}) \rightarrow H + O(^1D). \quad (26)$$

$O(^1D)$ atoms would not be formed from the secondary photolysis of OH(ads) in ASW after prolonged photoirradiation because the TOF spectrum of $O(^1D)$ for ASW after 30 min photoirradiation has the similar translational distribution to that of fresh H_2O_2 on ASW. Van Dishoeck and Dalgarno performed theoretical calculations of the photodissociation of the OH by *ab initio* calculations and predicted that the vuv photodissociation of OH at 152–190 nm would not lead to $O(^1D)+H$ but only to $O(^3P_J)+H$.[55,56] In fact, the secondary photolysis of OH(ads) is attributed to $O(^3P_J)$ formation in the 157 nm photolysis of water ice where the TOF spectra of $O(^3P_2)$ for ASW after prolonged photoirradiation have a different translational distribution from those of fresh ASW and fresh H_2O_2 on ASW. These results will be described in the following paper for our separate experiments.

The contribution of HO_2 would also be small since (a) the time evolution data of $O(^1D)$ in Fig. 2 are quite similar to those of H_2O_2 on the ice surface while HO_2 is produced from a three-step reaction of $OH+H_2O_2$ where H_2O_2 is produced from OH+OH, and (b) the concentration of HO_2 on/in ice disappeared or decreased at elevated temperatures such as 90 K.[10,57]

V. SUMMARY

We have demonstrated that electronically excited $O(^1D)$ atoms are formed via two processes: The unimolecular reaction on the surface of low temperature ASW at 90 K in the 157 nm photoirradiation and the bimolecular reactions of translationally and internally hot OH radicals on the surface of water ice. The hot OH radicals on ASW are produced from secondary photolysis of the photoproduct H_2O_2. In fresh ASW, the main part of $O(^1D)$ comes from the primary unimolecular reaction. In ASW after prolonged 157 nm photoirradiation, the contributions of unimolecular reaction become smaller, and the bimolecular reactions of hot OH radicals from the photoproduct H_2O_2 become dominant.

ACKNOWLEDGMENTS

The authors thank Professor H.-P. Loock of Queen's University for the simulation of the rotational spectra of OH radicals and Dr. S. Andersson of SINTEF Materials and Chemistry for fruitful discussions and comments. This work is supported by a grant-in-aid from JSPS (20245005).

[1] K. M. Pontoppidan, H. J. Fraser, E. Dartois, W.-F. Thi, E. F. van Dishoeck, A. C. A. Boogert, L. d'Hendecourt, A. G. G. M. Tielens, and S. E. Bisschop, Astron. Astrophys. **408**, 981 (2003).
[2] V. P. Zhdanov, Y. Ma, and T. Matsusima, Surf. Sci. **583**, 36 (2005).
[3] J. E. Roser, G. Vidal, G. Manico, and V. Pirronello, Astrophys. J. **555**, L61 (2001).
[4] N. Watanabe and A. Kouchi, Astrophys. J. **567**, 651 (2002).
[5] N. Watanabe, O. Mouri, A. Nagaoka, T. Chigai, and A. Kouchi, Astrophys. J. **668**, 1001 (2007).
[6] N. Watanabe and A. Kouchi, Prog. Surf. Sci. **83**, 439 (2008).
[7] L. J. Stief, W. A. Payne, and R. B. Klemm, J. Chem. Phys. **62**, 4000 (1975).
[8] A. Y. M. Ung, Chem. Phys. Lett. **28**, 603 (1974).
[9] M. Seki, K. Kobayashi, and J. Nakahara, J. Phys. Soc. Jpn. **50**, 2643 (1981).
[10] P. A. Gerakines, W. A. Schutte, and P. Ehrenfreund, Astron. Astrophys. **312**, 289 (1996).
[11] L. Khriachtchev, M. Pettersson, S. Jolkkonen, S. Pehkonen, and M. Rasanen, J. Chem. Phys. **112**, 2187 (2000).
[12] L. J. Stief and V. J. Decarlo, J. Chem. Phys. **50**, 1234 (1969).
[13] M. S. Westley, R. A. Baragiola, R. E. Johnson, and G. A. Baratta, Nature (London) **373**, 405 (1995).
[14] M. S. Westley, R. A. Baragiola, R. E. Johnson, and G. A. Baratta, Planet. Space Sci. **43**, 1311 (1995).
[15] K. I. Öberg, H. Linnartz, R. Visser, and E. F. van Dishoeck, Astrophys. J. **693**, 1209 (2009).
[16] G. A. Kimmel, R. G. Tonkyn, and T. M. Orlando, Nucl. Instrum. Methods Phys. Res. B **101**, 179 (1995).
[17] N. G. Petrik, A. G. Kavetsky, and G. A. Kimmel, J. Chem. Phys. **125**, 124702 (2006).
[18] A. Yabushita, D. Kanda, N. Kawanaka, M. Kawasaki, and M. N. R. Ashfold, J. Chem. Phys. **125**, 133406 (2006).
[19] A. Yabushita, T. Hama, D. Iida, N. Kawanaka, M. Kawasaki, N. Watanabe, M. N. R. Ashfold, and H. P. Loock, Astrophys. J. Lett. **682**, L69 (2008).
[20] A. Yabushita, T. Hama, D. Iida, N. Kawanaka, M. Kawasaki, N. Watanabe, M. N. R. Ashfold, and H. P. Loock, J. Chem. Phys. **129**, 044501 (2008).
[21] G. A. Kimmel and T. M. Orlando, Phys. Rev. Lett. **75**, 2606 (1995).
[22] A. Yabushita, Y. Inoue, T. Senga, M. Kawasaki, and S. Sato, J. Phys. Chem. B **106**, 3151 (2002).
[23] S. Sato, D. Yamaguchi, K. Nakagawa, Y. Inoue, A. Yabushita, and M. Kawasaki, Langmuir **16**, 9533 (2000).
[24] S. T. Pratt, P. M. Dehmer, and J. L. Dehmer, Phys. Rev. A **43**, 4702 (1991).
[25] N. Taniguchi, K. Takahashi, Y. Matsumi, S. M. Dylewski, J. D. Geiser, and P. L. Houston, J. Chem. Phys. **111**, 6350 (1999).
[26] M. E. Greenslade, M. I. Lester, D. C. Radenovic, A. J. A. van Roij, and D. H. Parker, J. Chem. Phys. **123**, 074309 (2005).
[27] F. M. Zimmermann and W. Ho, J. Chem. Phys. **100**, 7700 (1994).
[28] F. M. Zimmermann and W. Ho, Surf. Sci. Rep. **22**, 127 (1995).
[29] A. Yabushita, T. Hama, D. Iida, and M. Kawasaki, J. Chem. Phys. **129**, 014709 (2008).
[30] T. Hama, A. Yabushita, M. Yokoyama, M. Kawasaki, and S. Andersson, J. Chem. Phys. **131**, 054508 (2009).
[31] M. K. Karapet'yants and M. K. Karapet'yants, *Handbook of Thermodynamic Constants of Inorganic and Organic Compounds* (Ann Arbor-Humphrey Science, London, 1970).
[32] A. J. Matich, M. G. Bakker, D. Lennon, T. I. Quickenden, and C. G. Freeman, J. Chem. Phys. **97**, 10539 (1993).
[33] R. van Harrevelt and M. C. van Hemert, J. Phys. Chem. A **112**, 3002 (2008).
[34] E. J. Dunlea and A. R. Ravishankara, Phys. Chem. Chem. Phys. **6**, 3333 (2004).
[35] W. Zheng, D. Jewitt, and R. I. Kaiser, Phys. Chem. Chem. Phys. **9**, 2556 (2007).
[36] T. M. Orlando and G. A. Kimmel, Surf. Sci. **390**, 79 (1997).
[37] D. M. Chipman, J. Chem. Phys. **122**, 044111 (2005).
[38] D. M. Chipman, J. Chem. Phys. **124**, 044305 (2006).
[39] P. H. Hahn, W. G. Schmidt, K. Seino, M. Preuss, F. Bechstedt, and J. Bernholc, Phys. Rev. Lett. **94**, 037404 (2005).
[40] N. G. Petrik and G. A. Kimmel, Phys. Rev. Lett. **90**, 166102 (2003).
[41] N. G. Petrik and G. A. Kimmel, J. Chem. Phys. **121**, 3736 (2004).
[42] S. H. Mousavipour and V. Saheb, Bull. Chem. Soc. Jpn. **80**, 1901 (2007).
[43] L. Khriachtchev, M. Pettersson, S. Tuominen, and M. Rasanen, J. Chem. Phys. **107**, 7252 (1997).
[44] L. Schriver, C. Barreau, and A. Schriver, Chem. Phys. **140**, 429 (1990).
[45] S. Andersson, A. Al-Halabi, G.-J. Kroes, and E. F. van Dishoeck, J. Chem. Phys. **124**, 064715 (2006).
[46] S. Andersson and E. F. van Dishoeck, Astron. Astrophys. **491**, 907 (2008).
[47] I. C. Lu, F. Y. Wang, K. J. Yuan, Y. Cheng, and X. M. Yang, J. Chem. Phys. **128**, 066101 (2008).
[48] D. W. Hwang, X. F. Yang, and X. M. Yang, J. Chem. Phys. **110**, 4119 (1999).
[49] X. F. Yang, D. W. Hwang, J. J. Lin, and X. Ying, J. Chem. Phys. **113**, 10597 (2000).
[50] J. A. Dodd, S. J. Lipson, and W. A. M. Blumberg, J. Chem. Phys. **92**, 3387 (1990).
[51] C. Meredith, T. P. Hamilton, and H. F. Schaefer III, J. Phys. Chem. **96**, 9250 (1992).
[52] R. D. Bach, A. L. Owensby, C. Gonzalez, H. B. Schlegel, and J. J. W. McDouall, J. Am. Chem. Soc. **113**, 6001 (1991).
[53] J. Franz, J. S. Francisco, and S. D. Peyerimhoff, J. Chem. Phys. **130**, 084304 (2009).
[54] A. Yabushita, Y. Hashikawa, A. Ikeda, M. Kawasaki, and H. Tachikawa, J. Chem. Phys. **120**, 5463 (2004).
[55] E. F. van Dishoeck and A. Dalgarno, Astrophys. J. **277**, 576 (1984).
[56] E. F. van Dishoeck and A. Dalgarno, J. Chem. Phys. **79**, 873 (1983).
[57] C. Laffon, S. Lacombe, F. Bournel, and Ph. Parent, J. Chem. Phys. **125**, 204714 (2006).